Received: 12 May 2021 | Revised: 23 October 2021 | Accepted: 29 November 2021 | Published on: 6 April 2022

DOI: 10.1002/1438-390X.12124

Population Ecology WILEY

ORIGINAL ARTICLE

The transfer function method reveals how age-structured populations respond to environmental fluctuations with serious implications for fisheries management

Alexander Sadykov[1,2] | **Keith Farnsworth**[1] | **Dinara Sadykova**[3] | **Nils C. Stenseth**[2]

[1]School of Biological Sciences, Queen's University Belfast, Belfast, UK

[2]The Centre for Ecological and Evolutionary Synthesis, University of Oslo, Oslo, Norway

[3]UK Centre for Ecology & Hydrology, Wallingford, UK

Correspondence
Alexander Sadykov, School of Biological Sciences, Queen's University Belfast, 19 Chlorine Gardens, Belfast, BT9 5DL, UK.
Email: a.sadykov@qub.ac.uk

Funding information
Department of Agriculture, Food and the Marine, Grant/Award Number: 15/S/744

Abstract

Fluctuations in wild fish populations result from interaction between population dynamics and environmental forcing. Age-structured populations can magnify or dampen particular frequencies of these fluctuations, depending on life cycle and species traits. The transfer function (TF) gives a detailed analytical description of these phenomena. In this study, we derive a generalized form of TF to investigate the fluctuations of fish populations in response to species traits and environmental noise characteristics. We found that for semelparous species, fluctuations in fish stocks log-size are directly proportional to the recruitment elasticity and inversely proportional to the age of maturity, and for iteroparous species, fluctuations in fish stocks log-size are inversely proportional to the adult lifespan. In addition to the already known effect of cohort resonance (increased sensitivity to environmental fluctuations on cohort timescales in the elastic range of recruitment elasticity), we find a stock resonance effect (increased sensitivity to environmental fluctuations on double cohort timescales in the inelastic range of recruitment elasticity). These results were then applied to fisheries management. The relationship between fishing mortality and species-specific variability of fish stocks was formalized. In accordance with this analysis, precautionary levels for different catches were estimated.

KEYWORDS

age-structured population, cohort resonance, environment fluctuations, fish stock management, transfer function

1 | INTRODUCTION

Wild populations fluctuate, sometimes with enormous amplitude, the classic example being that of small pelagic fish (e.g., sardines and anchovies) (Schwartzlose et al., 1999). This is in part due to interactions with other populations, but also due to interaction with environmental variations (Hjort, 1914, 1926). These variations

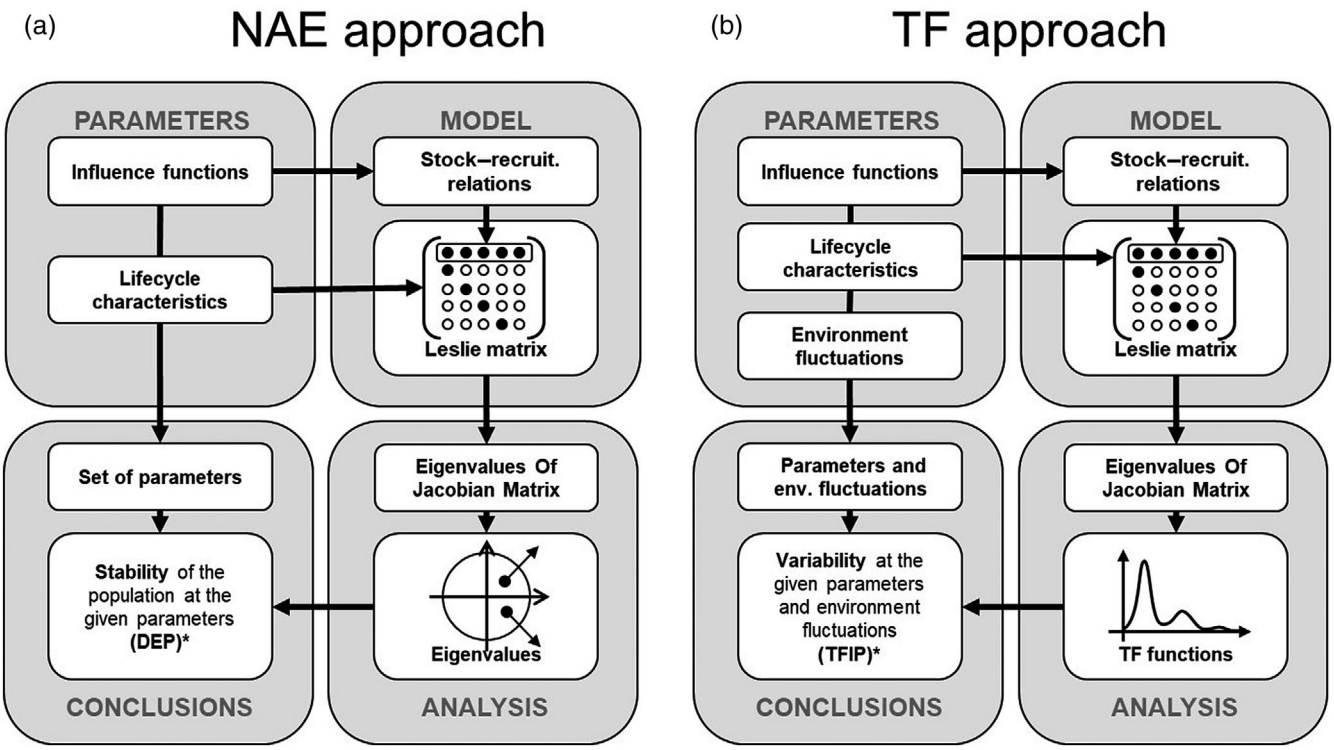

FIGURE 1 Block diagrams for (a) numerical analysis of the eigenvalues (NAE) and (b) transfer function (TF) approaches to the analysis of age-structured populations. *DEP is the dominant eigenvalue (contour) plot. *TFIP is the transfer function integral (contour) plot

can be periodic (e.g., the El Niño-Southern Oscillation [ENSO]—Chavez et al., 2003), or appear as random environmental forcing, especially, acting on recruitment, which can no longer be regarded as merely density-dependent (Solari et al., 2010). Modern fisheries management usually seeks to maintain fishing mortality within safe limits of maximum sustainable yield (MSY) by matching catching effort to population replacement, but this is fraught with difficulties as fish populations respond both to fishing mortality and natural sources of variation, particularly in recruitment. The effects are accumulated over the lives of the population members because, via growth and mortality, both size selective fishing and reproductive output are age-dependent, given any multi-annual life-history strategy (semelparous or iteroparous). Each cohort of the population makes its own contribution to the overall response to exogenous variability and its response propagates through time as the cohort matures. This way a multi-annual population acts as an autoregressive "filter" on the exogenous variation. The magnitude of these accumulated population variations can depend on the fishing pressure (Anderson et al., 2008; Hsieh et al., 2006) as this influences the relative size of age cohorts. Since MSY should not be exceeded, precautionary reference points (limits) are usually set, but in the absence of a thorough understanding of the mechanisms of variability and stock stability, these are typically heuristic (e.g., 2/3 F_{MSY} and $F_{0.1}$).

Recently, Willberg et al. (2019) introduced robust control theory (optimization taking account of worst-case values using likelihood calculations) to give precautionary reference points a quantitative justification, but that and similar efforts still depend on empirical estimates of expected variability, which is typically very difficult because of the dependence on catch and unknown environmental forcing. To develop beyond that requires an understanding of how wild population variability depends on catch levels and this is where a model of the propagation of variation through stock cohorts becomes valuable.

Over the past decades, several approaches to the analysis of age-structured populations under environment fluctuations have been proposed. These studies have shown that stability and variability are key characteristics that determine the behavior of such populations. To assess the stability, a method of numerical analysis of the eigenvalues (hereafter NAE) of the Jacobian matrix was developed (Botsford et al., 2019). This article develops a *transfer function* (TF) method that can be used to assess the variability of age-structured populations (Bjørnstad & Nisbet, 2004; Gross & de Roos, 2021).

The main structural components of both approaches are shown on Figure 1. As we can see, both methods have

the same model component (i.e., an age-structured Leslie matrix with density-dependent reproduction defined by the stock–recruitment relations [SRRs]); also, both methods have the same entry to the analytic component (i.e., finding the eigenvalues of the Jacobian matrix at equilibrium population size). From here, the paths of the methods diverge, the NAE method analyses the positions of the eigenvalues (especially the dominant eigenvalue) on the complex plane, whereas the TF method uses eigenvalues to transform the population dynamics into the form of a delay-coordinate time series. The Fourier transform of this gives the TF, which is a description of the response of the system (structured population) to any driving signal, in the "frequency domain." With the TF it is straightforward to incorporate any environmental fluctuations for given parameters and draw conclusions considering the spectral characteristics of the environment. It should be emphasized that the methods show different aspects of the dynamic behavior of populations. The NAE method reveals the stability of the population (the rate of convergence to equilibrium after a single disturbance), while the TF method reveals the variability of the population (quantifying the magnitude and spectrum of population fluctuations for any given constant spectrum of environmental noise). One advantage of the TF method is that it is then possible to estimate the expected variability and therefore uncertainty of, for example, fishery management targets such as MSY, as the stock responds to variability in the environment. We will show that this itself is a calculable function of the fishing mortality.

2 | DERIVATION OF TFs

To accommodate a wide range of population structures (e.g., life-history strategies), we will consider an age-structured population with a range of different density-dependent stock–recruitment models (SRRs), in the presence of a fluctuating environment under harvesting pressure; all with fisheries management in mind. The analytical derivation of a general form of the TF and the investigation of its properties, depending on the parameters of the population (including harvesting), presents both practical and theoretical interests. Here we aim to derive explicit TF expressions, which apply generally for any life history strategy and any SRR. This will provide general flexibility in studying stock variability analytically that is, without using extensive numerical simulations. On this basis, it can be developed into a practical tool for fishery management. The TF is *intrinsic* to the dynamic system, fully characterizing the response of the system to any input. The TF is a character of a linear system, so to calculate a TF we need the equilibrium solution to the age-structured population dynamic, which we must linearize and find the log-transformed deviation from equilibrium. This is set up as follows.

2.1 | General age-structured population dynamics model

Consider an annually reproducing (iteroparous) species with age-structured population represented by the vector $\mathbf{N_t}(N_{0,t},...,N_{d,t})$, where $N_{j,t}$ is j-th age cohort abundance at time t or equivalently in another notation by $\mathbf{N}(t)=(N_1(t),...,N_d(t))$. The population dynamic equations for density-dependent recruitment with temporal environmental noise ε_t can be written in the difference equation (or delay-coordinate) form as:

$$\begin{aligned} N_{0,t} &= \varepsilon_t \cdot R(S_t) \\ N_{j,t} &= \lambda_j \cdot N_{j-1,t-1}, \end{aligned} \tag{1}$$

or in equivalent matrix form as

$$\begin{bmatrix} N_1(t+1) \\ N_2(t+1) \\ \dots \\ N_d(t+1) \end{bmatrix} = \begin{bmatrix} \varepsilon(t) \cdot R(S(t)) \\ \lambda_1 \cdot N_1(t) \\ \dots \\ \lambda_d \cdot N_{d-1}(t) \end{bmatrix}, \tag{2}$$

where λ_i are age-specific survival rates, $R(S_t)$ is an SRR and $S(t)=\sum_{j=1}^{d} v_j \cdot N_j(t)$ is the *spawning power of the population* represented by a weighted sum of cohort abundances and *reproductive qualities* $\nu_i (0 \le \nu_i \le 1)$ to take account of differences in per-capita contributions of each cohort to spawning stock. These differences can reflect the differences in quality and quantity of eggs (Hixon et al., 2014), as well as the differences in proportion of spawners among cohorts. In the case of equal reproductive qualities $\forall \nu_i = 1$, the spawning power is equal to spawning stock size $s(t)=\sum_{j=1}^{d} N_j(t)$. It should be noted that for reproductive qualities the term *influence function* (Botsford et al., 2019) is also used, usually in the form of a pair of functions, one of which is responsible for egg production and the other for egg survival. Hereinafter, for convenience, we do not split it into two separate functions.

2.2 | Elasticity of recruitment–stock relations

Without loss of generality, the SRR $R(S)$ can be represented as some combination of linearly increasing and

nonlinearly decreasing parts as $R(S) \equiv a \cdot S \cdot F(S/K)$, where the nonlinear monotonic function $F(z) : \mathbb{R}^+ \to \mathbb{R}^+$ satisfies the conditions $F(z) > 0$, $dF(z)/dz < 0$, and parameters a and K are chosen in such a way that $F(0) \equiv 1$. These increasing and decreasing parts are sometimes interpreted as *linear egg production* and *nonlinear density-dependent egg survival functions* (the term *recruitment survival function* is used as well) (Botsford et al., 2019); here we take a more cautious approach and refer $F(z)$ as a *specific recruitment function* without going to details of eggs and larvae related processes. For historical reason, parameter K is often called a *carrying capacity*, because similar density-dependent relations are widely used in unstructured population dynamics. Hereafter, we reluctantly accept this term, but note that in the present analysis it is just a *stock size scale parameter* in the specific recruitment function $F(z)$, where $z \equiv S/K$. The parameter a is the slope of the function $R(S)$ at zero (since $F(0) \equiv 1$) and can be interpreted as the maximum number of recruits that one individual can produce during one spawning. In the literature, this parameter is also referred as a *coefficient of the SRR* and/or a *proliferation rate* (Myers et al., 1999). We can also consider $R(S)$ as total recruitment (i.e., total contribution of all spawners to the next generation) and find marginal recruitment (i.e., individual contribution of each spawner) as $\frac{\partial R(z)}{\partial z} = a \cdot K \cdot F(z) + a \cdot z \cdot K \cdot \frac{\partial}{\partial z} F(z) = a \cdot K \cdot F(z) \cdot \left(1 + E_R(z)^{-1}\right)$, where $E_R(z) = \frac{\partial z/z}{\partial F/F} = \frac{F(z)}{z} \cdot \frac{\partial z}{\partial F(z)} = \frac{\partial \ln(z)}{\partial \ln(F(z))}$ is the *recruitment elasticity* of the stock (or recruitment–stock elasticity). The recruitment elasticity is a measure of responsiveness of the stock size to a change in the recruitment. The following descriptive terms apply: in the *elastic range* of recruitment elasticity, small changes in recruitment cause relatively large changes in the population stock size; in the *inelastic range*, changes in recruitment cause relatively small changes in the population stock size. In the fishery literature, these are often termed *compensatory* and *overcompensatory* ranges of SRR (respectively). It should be noted that the inverse value of the recruitment–stock elasticity is a *stock–recruitment elasticity* $E_R(z)^{-1} = \frac{z}{F(z)} \frac{\partial F(z)}{\partial z} = E_S(z)$, which is often (confusingly) denoted as "K" (note that this K is not related to carrying capacity) and is widely used in the fishery literature under the name of *a normalized slope of the recruitment survival function* (Botsford et al., 2019).

The recruitment elasticity is always negative, since $F(z)$ is a monotonically decreasing function of the stock sizes, whereas the stock–recruitment sensitivity can be either negative (if the absolute value of recruitment elasticity is less than 1), or positive (if the absolute value of recruitment elasticity is greater than 1). Significantly, some SRRs are always elastic (e.g., Cushing and Beverton–Holt SRR), while others may have both inelastic and elastic ranges (e.g., Ricker and Maynard–Smith–Slatkin SRR).

2.3 | Equilibrium cohorts and stock sizes

The equilibrium population sizes for the model (1 and 2) can be found by balancing the recruitment and other life history processes, as follows. At the equilibrium point, the abundance of i-th age cohort is $\widehat{N}_i = \prod_{j=1}^{i} \lambda_j \cdot \widehat{N}_0$ (using hat notation to denote quantities at equilibrium) and $\widehat{N}_0$ is equilibrium zero-cohort size, the equilibrium spawning power is $\widehat{S} \equiv L \cdot \widehat{N}_0$, where the quantity $L \equiv L(d, \overline{\lambda}, \overline{\nu}) = \sum_{i=1}^{d} \nu_i \cdot \prod_{j=1}^{i} \lambda_j$ is the *life-time reproductive potential* (LRP). In the case of equal reproductive quality (i.e., $\forall \nu_i = 1$), the equilibrium spawning stock size $\widehat{s} \equiv l \cdot \widehat{N}_0$, where $l \equiv l(d, \overline{\lambda}) = L(d, \overline{\lambda}, \forall \nu_i = 1) = \sum_{i=1}^{d} \cdot \prod_{j=1}^{i} \lambda_j$.

The equilibrium zero-cohort population can be calculated using an inverse SRR function F^{-1} throughout, as $\widehat{N}_0 = F^{-1}\left(\frac{1}{a \cdot L}\right) \cdot \frac{K}{L}$. Then the equilibrium spawning stock size and equilibrium spawning power are $\widehat{s} = l \cdot \widehat{N}_0 = F^{-1}\left(\frac{1}{a \cdot L}\right) \cdot K \cdot \frac{l}{L}$ and $\widehat{S} = L \cdot \widehat{N}_0 = F^{-1}\left(\frac{1}{a \cdot L}\right) \cdot K$, respectively. Note that in the case of equal cohort reproductive qualities: $L = l$ and $\widehat{S} = \widehat{s}$.

2.4 | Life-time reproductive potential

The quantity L summarizes the schedules of several mutually interconnected vital processes within population: survival, maturation, growth, reproduction, and senescence (i.e., additional age-related mortality). To illustrate this point let us consider a population with a simple life cycle consisting of m immature and $d - m$ mature cohorts, which has survival rates λ_y and λ_s accordingly. In this case, the combination $L = \left(\lambda_y{}^m\right) \cdot \left(\frac{1}{1-\lambda_s}\right) \cdot \left(1 - \lambda_s{}^{d-m+1}\right)$ can be interpreted as the lifetime reproductive potential (LRP) of the individual, since it is the probability to reach adulthood ($\lambda_y{}^m$) multiplied by adulthood (reproductive) lifespan ($1/(1-\lambda_s)$) and accounting for senescence with the term ($1 - \lambda_s{}^{d-m+1}$). In other words, this value can be understood as the expected number of reproduction events that an individual has during her lifespan. In turn, the value $a \cdot L$ can be interpreted as a *lifetime reproductive success* (LRS) (i.e., expected numbers of recruits that the individual can produce during her lifespan), since it is the proliferation rate multiplied by the lifetime reproductive potential. Accordingly, the necessary condition for survival of population is $a \cdot L \geq 1$. Tables 1 and 2 give particular examples of calculating value of L for different life cycles and equilibrium population sizes for commonly used SRR.

TABLE 1 Life-time reproductive potential (LRP) for different lifecycle models (in order of decreasing complexity and generality)

Cohort structure of the stock	Cohort reproductive quality ν_i	Survival λ_j	Life-time reproductive potential L
d cohorts	Different for each cohort	Different for each cohort	$L(d,\overline{\lambda},\overline{\nu}) = \sum_{i=1}^{d} \nu_i \cdot \prod_{j=1}^{i} \lambda_j$
d cohorts	The same for each cohort	Different for each cohort	$L(d,\overline{\lambda}) \equiv l(d,\overline{\lambda}) = \sum_{i=1}^{d} \prod_{j=1}^{i} \lambda_j$
m immature and $d-m$ adult cohorts	Zero for immature and 1 for adult contorts	Different for each cohort	$L(d,m,\overline{\lambda}) = \prod_{j=1}^{m} \lambda_j \cdot \sum_{i=m}^{d} \prod_{j=1}^{i} \lambda_j$
m immature and $d-m$ adult cohorts	Zero for immature and 1 for adult contorts	λ_y for immature and λ_s for adult cohorts	$L(d,m,\lambda_s,\lambda_y) = \frac{{\lambda_y}^m \cdot \left(1-{\lambda_s}^{d-m+1}\right)}{(1-\lambda_s)}$
m immature and infinite number of adult cohorts	Zero for immature and 1 for adult contorts	λ_y for immature and λ_s for adult cohorts	$L(m,\lambda_s,\lambda_y) \equiv L_\infty = \frac{{\lambda_y}^m}{(1-\lambda_s)}$
m immature and a single adult cohort (semelparous species)	Zero for immature and 1 for adult contort	λ_y for immature and zero for adult cohort	$L(m,\lambda_y) \equiv L_s = {\lambda_y}^m$

TABLE 2 Basic characteristics of the age-structured models for different stock-recruitment relations

	Cushing model	Beverton–Holt model	Moran–Ricker model	Maynard–Smith, Slatkin model
Stock-recruitment relation	$a \cdot S_t \cdot (S_t/K)^{-\beta}$	$\frac{a \cdot S_t}{1+S_t/K}$	$a \cdot S_t \cdot e^{-S_t/K}$	$\frac{a \cdot S_t}{1+(S_t/K)^{\beta}}$
Equilibrium zero-cohort size	$\left(a \cdot L^{(1-\beta)}\right)^{1/\beta} \cdot K$	$(a \cdot L - 1) \cdot K/L$	$\ln(a \cdot L) \cdot K/L$	$(a \cdot L - 1)^{1/\beta} \cdot K/L$
Equilibrium stock size	$\left(a \cdot L^{(1-\beta)}\right)^{1/\beta} \cdot K \cdot l$	$(a \cdot L - 1) \cdot K \cdot l/L$	$\ln(a \cdot L) \cdot K \cdot l/L$	$(a \cdot L - 1)^{1/\beta} \cdot K \cdot l/L$
Elasticity at equilibrium	$-1/\beta$	$-a \cdot L/(a \cdot L - 1)$	$-1/\ln(a \cdot L)$	$-a \cdot L/(\beta \cdot (a \cdot L - 1))$

Note: Note that in cases of Cushing and Beverton–Holt models, SRR are always elastic $|E_R| > 1$ (i.e., an increase of numbers of spawners leads to increase of numbers of recruits), while in cases of Ricker and Maynard–Smith and Slatkin models, SRR may be inelastic $|E_R| < 1$ at large value of LRS.

2.5 | Linearization around equilibrium

Following the standard procedure, we begin the derivation of the TF with the log-transformation of cohort abundances. After log-transformation and renaming $n_j(t) \equiv \ln\left(N_j(t)\right)$, Equations (1) and (2) can be rewritten as

$$\begin{aligned} n_{0,t} &= \ln \varepsilon_t + \ln a + \ln\left(F(S_t/K)\right) + \ln\left(S_t\right) \\ n_{j,t} &= \ln \lambda_j + n_{j-1,t-1}, \end{aligned} \tag{3}$$

or in equivalent matrix form as

$$\begin{bmatrix} n_1(t+1) \\ n_2(t+1) \\ \dots \\ n_d(t+1) \end{bmatrix} = \begin{bmatrix} \ln a + \ln\left(F(S(t)/K)\right) + \ln\left(S(t)\right) \\ \ln \lambda_1 + n_1(t) \\ \dots \\ \ln \lambda_d + n_{d-1}(t) \end{bmatrix} + \begin{bmatrix} \ln \varepsilon(t) \\ 0 \\ \dots \\ 0 \end{bmatrix}, \tag{4}$$

where $S(t) = \sum_{j=1}^{d} \nu_j \cdot e^{n_j(t)}$.

Further, a linear expansion around the equilibrium point gives the next non-homogenous first-order matrix equation for the dynamics of deviations of log-abundances from equilibrium, taken at the expected value of $\ln\varepsilon(t)$:

$$\mathbf{x}(t+1) = \mathbf{J} \cdot \mathbf{x}(t) + \mathbf{A} \cdot \theta(t), \tag{5}$$

where the deviation vectors are $\mathbf{x}(t) = \mathbf{n}(t) - \widehat{\mathbf{n}}(t)$ and $\theta(t) = \ln\varepsilon(t) - \ln\widehat{\varepsilon}$. The matrix $\mathbf{J}$ is the Jacobian matrix with elements: $J_{j,k} = \frac{\partial \widehat{n}_j}{\partial n_k}$, and the vector A is the partial derivative with respect to the stochastic term $A_j = \frac{\partial \widehat{n}_j}{\partial \ln(\varepsilon)}$ (which in this case has only one non-zero element $A_0 = \frac{\partial \widehat{n}_0(t)}{\partial \ln(\varepsilon)} = 1$). The non-zero elements of the Jacobian matrix are $J_{j,j-1} = \frac{\partial \widehat{n}_j}{\partial \widehat{n}_{j-1}} = 1$, $J_{0,k} = \frac{\partial \widehat{n}_0}{\partial n_k} = (1 + {E_R}^{-1}) \cdot P_k$, hence the Jacobian matrix can be rewritten as:

TABLE 3 Transfer functions for individual cohorts (j) and the stock (S), for each of three stock-recruitment relations

Cushing (density-dependent recruitment) model:	
$T_j(f) = \frac{1}{1-(1-\beta)\sum_{k=m}^{d} P_k \cdot e^{-2\pi i k f}}$	$\lim_{d\to\infty} \to \frac{\left(e^{2\pi i f}-\lambda_s\right)}{\left(e^{2\pi i f}-\lambda_s\right)-(1-\beta)\cdot(1-\lambda_s)\cdot e^{-2\pi i f(m-1)}}$
$TS(f) = \frac{\sum_{k=m}^{d} P_k \cdot e^{-2\pi i k f}}{1-(1-\beta)\sum_{k=m}^{d} P_k \cdot e^{-2\pi i k f}}$	$\lim_{d\to\infty} \to \frac{(1-\lambda_s)\cdot e^{-2\pi i f(m-1)}}{\left(e^{2\pi i f}-\lambda_s\right)-(1-\beta)\cdot(1-\lambda_s)\cdot e^{-2\pi i f(m-1)}}$
Beverton–Holt (density-dependent recruitment) model:	
$T_j(f) = \frac{a\cdot L}{a\cdot L-\sum_{k=m}^{d} P_k \cdot e^{-2\pi i k f}}$	$\lim_{d\to\infty} \to \frac{a\cdot {\lambda_y}^m\cdot\left(e^{2\pi i f}-\lambda_s\right)}{a\cdot {\lambda_y}^m\cdot\left(e^{2\pi i f}-\lambda_s\right)-(1-\lambda_s)^2\cdot e^{-2\pi i f(m-1)}}$
$TS(f) = \frac{a\cdot L\cdot\sum_{k=m}^{d} P_k \cdot e^{-2\pi i k f}}{a\cdot L-\sum_{k=m}^{d} P_k \cdot e^{-2\pi i k f}}$	$\lim_{d\to\infty} \to \frac{a\cdot {\lambda_y}^m\cdot(1-\lambda_s)\cdot e^{-2\pi i f(m-1)}}{a\cdot {\lambda_y}^m\cdot\left(e^{2\pi i f}-\lambda_s\right)-(1-\lambda_s)^2\cdot e^{-2\pi i f(m-1)}}$
Moran–Ricker (density-dependent recruitment) model:	
$T_j(f) = \frac{1}{1-(1-\ln(a\cdot L))\sum_{k=m}^{d} P_k \cdot e^{-2\pi i k f}}$	$\lim_{d\to\infty} \to \frac{\left(e^{2\pi i f}-\lambda_s\right)}{\left(e^{2\pi i f}-\lambda_s\right)-(1-\ln(a\cdot L_\infty))\cdot(1-\lambda_s)\cdot e^{-2\pi i f(m-1)}}$
$TS(f) = \frac{\sum_{k=m}^{d} P_k \cdot e^{-2\pi i k f}}{1-(1-\ln(a\cdot L))\sum_{k=m}^{d} P_k \cdot e^{-2\pi i k f}}$	$\lim_{d\to\infty} \to \frac{(1-\lambda_s)\cdot e^{-2\pi i f(m-1)}}{\left(e^{2\pi i f}-\lambda_s\right)-(1-\ln(a\cdot L_\infty))\cdot(1-\lambda_s)\cdot e^{-2\pi i f(m-1)}}$

Note: In the functions, the weights $P_k = \widetilde{N}_k/\widetilde{S} = \lambda_y^m\cdot\lambda_s^{k-m}/L$, the life-time reproductive potential $L = {\lambda_y}^m\cdot\left(1-{\lambda_s}^{d-m+1}\right)/(1-\lambda_s)$ and $L_\infty = {\lambda_y}^m/(1-\lambda_s)$. The limits in the absence of senescence ($d\to\infty$) are also given.

$$\mathbf{J} = \begin{bmatrix} (1+{E_R}^{-1})\cdot P_1 & (1+{E_R}^{-1})\cdot P_2 & \cdots & (1+{E_R}^{-1})\cdot P_d \\ 1 & 0 & \cdots & 0 \\ 0 & 1 & \cdots & 0 \\ \vdots & \vdots & \ddots & \vdots \\ 0 & 0 & \cdots & 0 \end{bmatrix}, \tag{6}$$

where $P_k = \frac{\nu_k\cdot\prod_{j=1}^{k}\lambda_j}{L}$ is the relative contribution of the k-th cohort to reproduction (if all cohorts reproductive quality are equal $\forall\nu_k\equiv 1$, this quantity is the proportion of k-th cohort in the stock) and $E_R \equiv E_R(a\cdot L) = \left(\frac{\partial F(z)/F(z)}{\partial z/z}\Big|_{z=F^{-1}(1/aL)}\right)^{-1}$ is the recruitment elasticity of stock–recruitment curve in the equilibrium point, which in turn depends only on LRS. Using P_k, we can calculate the *generation time* or *mean age of reproduction* as $T_{age} = \sum_{k=1}^{d} k\cdot P_k$.

2.6 | Delay-coordinate representations and Fourier transformation

The matrix difference Equation (5) can be transformed to a single variable delay equation. Using the characteristic equation for the Jacobian matrix (6) $\lambda^d - (1+{E_R}^{-1})\cdot\sum_{k=1}^{d} P_k\cdot\lambda^{d-k} = 0$, we can derive delay-coordinate representations (Royama, 1992) for each of the cohort and for the stock log-size deviations as:

$$\begin{aligned} x_{j,t} &= c_j + \left(1+{E_R}^{-1}\right)\cdot\sum_{k=1}^{d} P_k\cdot x_{j,t-k} + \theta_t \\ s_t &= c + \left(1+{E_R}^{-1}\right)\cdot\sum_{k=1}^{d} P_k\cdot s_{t-k} + \sum_{k=1}^{d} P_k\cdot\theta_{t-k}. \end{aligned} \tag{7}$$

These equations represent population dynamics in the form of time series (ARMA process). In order to obtain a frequency representation, we can apply Fourier transformation to both parts of each equation and, after basic rearrangement get $\widetilde{x}(f) = T_j(f)\widetilde{\theta}(f)$ and $\widetilde{s}(f) = TS(f)\widetilde{\theta}(f)$, where $\widetilde{x}(f)$, $\widetilde{s}(f)$, and $\widetilde{\theta}(f)$ are the spectral functions of individual cohort, stock, and environment fluctuations, respectively. In turn, the TFs for the j-th cohort $T_j(f)$ and the whole spawning stock $TS(f)$, respectively, are

$$T_j(f) = \frac{1}{1-\left(1+E_R(a\cdot L)^{-1}\right)\cdot\sum_{k=1}^{d} P_k\cdot e^{-2\pi i k f}}, \tag{8}$$

TABLE 4 Comparative characteristics of cohort and stock resonances

	Cohort resonance	Stock resonance
Location relative to other regimes	At the boundary between stable and population extinction regimes	At the boundary between stable and unstable nonlinear regimes
Recruitment elasticity range	Elastic (compensatory)	Inelastic (overcompensatory)
Frequency characteristics of population fluctuations	There are no specific resonance frequencies; however, there is an amplification of low frequencies and frequencies close to the inverse generation time $1/T_{age}$	There is specific resonance frequency $f_{res} = 1/(\delta \cdot T_{age})$, where the parameter δ lies in the range $1.9 < \delta < 2.4$
Occurrence	Consistent, monotonically increasing with harvesting	Irregular, may appear or disappear with increasing harvesting
Correlations with environment fluctuations	Significant	Low or insignificant
Response to "red shift" in environment fluctuations	Increases	Decreases
Response to "blue shift" in environment fluctuations	Decreases	Increases

$$TS(f) = \frac{\sum_{k=1}^{d} P_k \cdot e^{-2\pi i k f}}{1 - \left(1 + E_R (a \cdot L)^{-1}\right) \cdot \sum_{k=1}^{d} P_k \cdot e^{-2\pi i k f}}. \quad (9)$$

Hereinafter we consider their general properties, some special cases and the application to the management of fish stocks, of these TFs. In Table 3, we present some examples of TFs for commonly used in fishery management SRR and life cycles.

3 | GENERAL PROPERTIES OF THE TFs

General equations (8) and (9) show that the behavior of these functions is defined by elasticity at equilibrium $E_R(a \cdot L)$ and weighted (by cohort's relative contribution to stock) time-delay series $\sum_{k=1}^{d} P_k \cdot e^{-2\pi i k f}$, subsequently, they can be calculated for specific frequencies 0 and 1/2 as 1 and $\sum_{k=1}^{d} (-1)^{k+1} P_k$, which gives the value of TFs at low and high frequency limits: $TS(0) = -E_R(a \cdot L) \equiv -E_R$ and $TS(1/2) = \frac{\sum_{k=1}^{d} (-1)^{k+1} P_k}{1 - \left(1 + E_R^{-1}\right) \cdot \sum_{k=1}^{d} (-1)^{k+1} P_k}$.

Significantly, these TFs can rise to infinity at certain frequencies, that is, produce a resonance ("true resonance," not mere amplification of environmental noise). The resonance conditions are fulfilled when the denominator of the TF becomes zero, the necessary conditions for this are: the imaginary part of the series is zero $\mathrm{Im}\left(\sum_{k=1}^{d} P_k \cdot e^{-2\pi i k f}\right) = 0$ and the real part is $\mathrm{Re}\left(\sum_{k=1}^{d} P_k \cdot e^{-2\pi i k f}\right) = \frac{E_R}{1+E_R}$. Therefore, the spectral characteristic of the TF is determined by the distribution of reproductive cohorts within stock. We can estimate an effective number (Hill, 1973) of reproductive cohorts as an *inverse diversity index*.

$N_{eff} = \left(\sum_{k=1}^{d} P_k^2\right)^{-1} = L^2 \cdot \left(\sum_{k=1}^{d} \nu_k^2 \cdot \prod_{j=1}^{k} \lambda_j^2\right)^{-1}$ or as a *degree of iteroparity* $It = \exp\left(-\sum_{k=1}^{d} P_k \cdot \ln P_k\right)$ (Paniw et al., 2018). It can be seen that $N_{eff} \sim L^2$, which means that populations with low lifetime reproduction potential consist of few reproductive cohorts, while a high value of LRP implies the presence of numerous approximately even productive cohorts.

Given this, we can now consider TFs in two extreme (bounding) cases:

1. *Semelparous limit*, where LRP is sufficiently small $L \to L_s = \lambda_y < 1$, therefore, a single productive cohort dominates in the stock, which implies that $P_k \to 1$ for this cohort and $P_i \to 0$ for all other cohorts.
2. *Iteroparous limit*, where LRP tends toward infinity $L \to L_\infty = \lambda_y/(1 - \lambda_s) \to \infty$, while adult survival rate tends to 1, which implies that the stock consists of many equally productive cohorts.

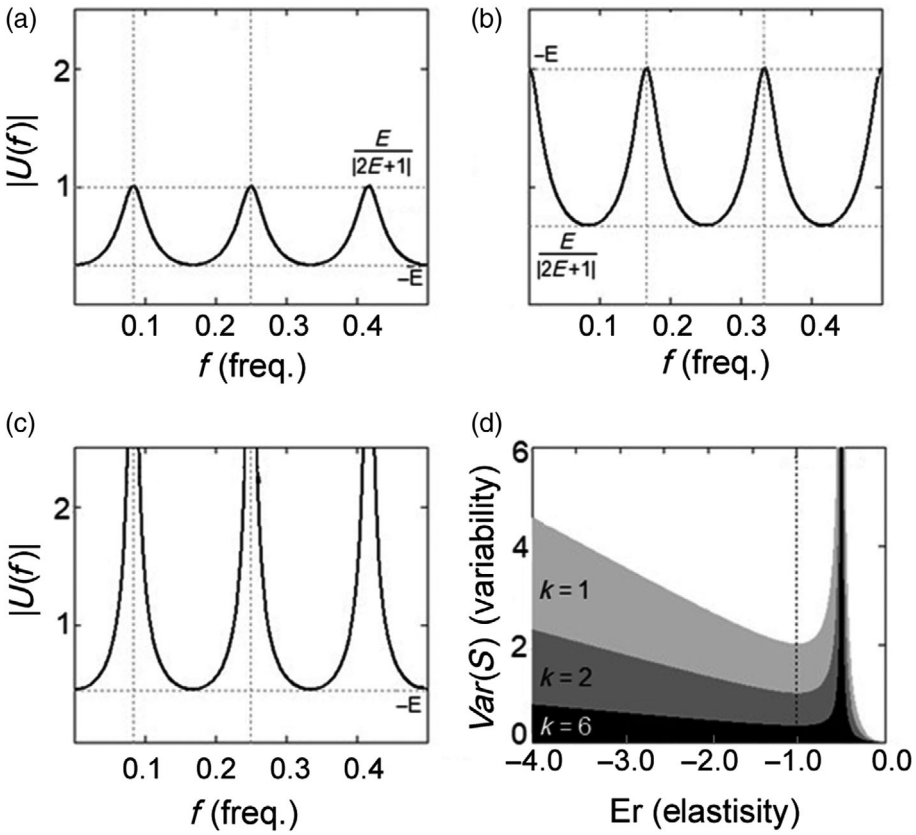

FIGURE 2 Universal transfer function (UTF) over different ranges of SRR elasticity: (top left (a)) inelastic range $|E_R| = 1/3$; (top right (b)) elastic range $|E_R| = 2$; (bottom left [c]) stock resonance range $|E_R| = 0.45$. Bottom right panel (d) shows total variability of stock for UTF at different elasticities and maturation ages k [1, 2, 6]

Then, knowing the behavior of the TF in these limits, we can estimate the TF over the entire range of parameters.

3.1 | TF at the semelparous limit

In the semelparous limit, the stock TF (9) converges to what we will call a *universal transfer function* (UTF):

$$TS(f) \underset{P_k \to 1}{\to} UTS(f) = \frac{1}{e^{2\pi i \widetilde{k} f} - (1 + E_R{}^{-1})}, \qquad (10)$$

where $\widetilde{k}$ is age of single productive cohort (in case of equal reproductive qualities, it equals to age of the first mature cohort $\widetilde{k} = m$). The UTF does not explicitly depend on type of SRR (hence our terming it "universal") and, due to its simplicity, makes it possible to identify key features of the spectral behavior (Figure 2). (1) Within the elastic range of SRR ($|E_R| > 1$), the UTF is a periodic function with maximum value $-E_R$ at frequencies $f_n = \frac{n}{\widetilde{k}}, n = 0, ..., [k/2]$ and minimum value $\frac{-E_R}{|2E_R - 1|}$ at frequencies $f_n = \frac{2n+1}{2\widetilde{k}}, n = 0, ..., [k/2]$. (2) Within the inelastic range ($|E_R| < 1$), the UTS flips over with maximum value $\frac{-E_R}{|2E_R - 1|}$ at frequencies $f_n = \frac{2n+1}{2\widetilde{k}}, n = 0, ..., [k/2]$ and minimum value $-E_R$ at frequencies $f_n = \frac{n}{\widetilde{k}}, n = 0, ..., [k/2]$. (3) At a specific value of elasticity $E_R = -1/2$, UTS undergoes resonance (i.e., maximum value of TF reaches infinity at $1/2\widetilde{k}$ frequency). The total variability of stock log-size for a UTF (with uncorrelated environmental noise) can be calculated explicitly as a double integral of the power spectrum over the frequency domain:

$$VarS \sim 2 \cdot \int_0^{1/2} |UTF(f)|^2 df = \frac{E_R{}^2}{\widetilde{k} \cdot |2E_R + 1|}. \qquad (11)$$

This equation shows that the variability has a local minimum at unit elasticity $|E_R| = 1$. With a deviation in the direction of greater elasticity ($|E_R| > 1$), Equation (11) can be approximated by the simple linear relation $VarS \sim \frac{|E_R|}{2 \cdot \widetilde{k}}$, which can be restated in biological terms as "for semelparous species, the variation in stock size is directly proportional to the recruitment elasticity of the SRR and inversely proportional to the age of maturity." On the other hand, a deviation in the direction of greater inelasticity ($|E_R| \to 1/2$) leads to a singularity where the variability tends to infinity. In the next section, we analyze variability and stability together and relate these raises in variability to the phenomena of *cohort resonance* (Bjørnstad & Nisbet, 2004; Botsford et al., 2014) and *stock resonance* (Supporting Information 1).

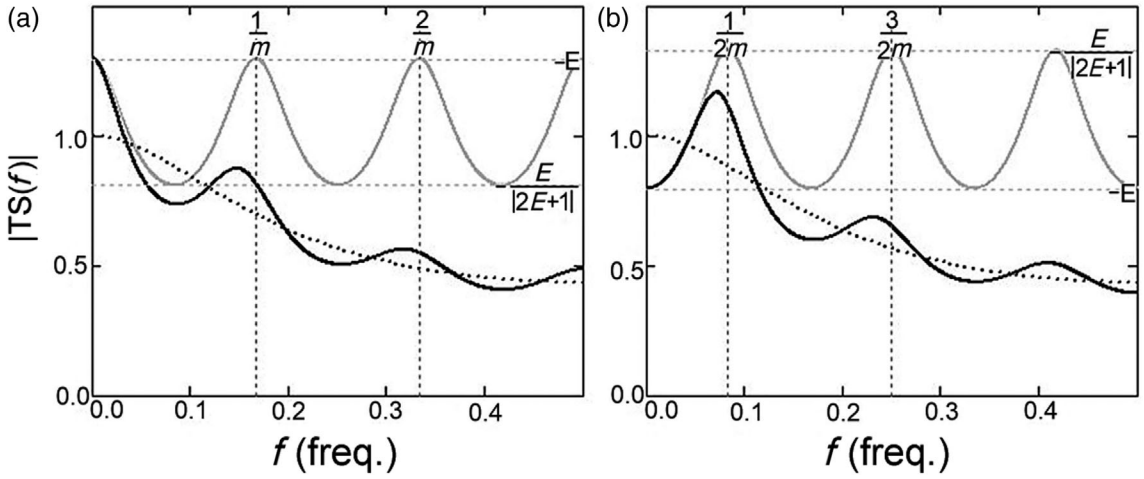

FIGURE 3 Transfer function (black line) and its asymptotic behaviors: (1) at semelparous limit or low LRP (gray line), where transfer function converges to UTF; (2) at iteroparous limit or high LRP (dotted line). Left panel (a) for elastic range of SRR $|E_R| = 1.3$, right panel (b) for inelastic range of SRR $|E_R| = 0.8$

3.2 | TF at the iteroparous limit

In the iteroparous limit, the time-delay series becomes relatively small, and the stock TF (9) can be estimated as $TS(f) \to ITS(f) = \sum_{k=1}^{d} P_k \cdot e^{-2\pi i k f}$. Further, in the case of survival rates being equal for all adult cohorts $\forall \lambda_j = \lambda_s$, we find an approximation for an iteroparous TF:

$$ITS(f) \sim \frac{1-\lambda_s}{\sqrt{\lambda s^2 - 2\cdot\lambda_s \cos(2\pi\cdot f)+1}}. \quad (12)$$

The variability of stock size in this case can be calculated as

$$VarS \sim 2\cdot \int_0^{1/2} |ITS(f)|^2 df = \frac{1-\lambda_s}{1+\lambda_s} = \frac{1}{2\cdot\tau - 1}, \quad (13)$$

where $\tau \equiv 1/(1-\lambda_s)$ is the expected adult lifespan. This result can be rephrased as: "variation in stock size tends to increase with decreasing adult lifespan," or equivalently as "for iteroparous species, the variation in fish stock log-sizes is inversely proportional to adult lifespan." Combining asymptotic behavior of TFs in both limits (Figures 2 and 3), we can conclude in general that

1. an increase in the number of adult cohorts leads to a decrease in the effect of high-frequency fluctuations on the stock variations (Figure 3 shows that the TF becomes closer to the dotted line);
2. cohort resonance can be manifested at elastic range of recruitment elasticity and low degree of iteroparity (the left panel of Figure 3 shows that the TF becomes closer to the gray line);
3. there is general tendency to increase the stock variations with decreasing degree of iteroparity, but this tendency can be broken at inelastic range of recruitment elasticity by the stock resonance (Figure 3 shows that the TF becomes closer to the gray line, but the bottom right panel of Figure 2 shows a resonance peak in the inelastic range).

4 | STABILITY AND VARIABILITY OF AGE-STRUCTURED POPULATIONS

In this section, we show how to evaluate the population stability (i.e., the rate at which it returns to equilibrium after a single perturbation) and variability (i.e., the integrated spectral power of population variation undergoing persistently fluctuating environmental forcing). Population stability can be determined by the magnitude of the dominant eigenvalue(s) of the Jacobian matrix (i.e., by the NAE method), and population variability can be determined by the integral over frequency space of the product of TF and the noise power spectrum (Supporting Information 2) (Ripa et al., 1998; Ripa & Lundberg, 1996; Schmidt et al., 2018). A comprehensive interpretation of system behavior requires assessing both stability and variability for a biologically meaningful range of parameters. For these purposes, we have developed two supporting tools that help visualize the results: (1) The dominant eigenvalue (contour) plot (DEP), which shows the magnitude of the maximum eigenvalue(s) of the Jacobian

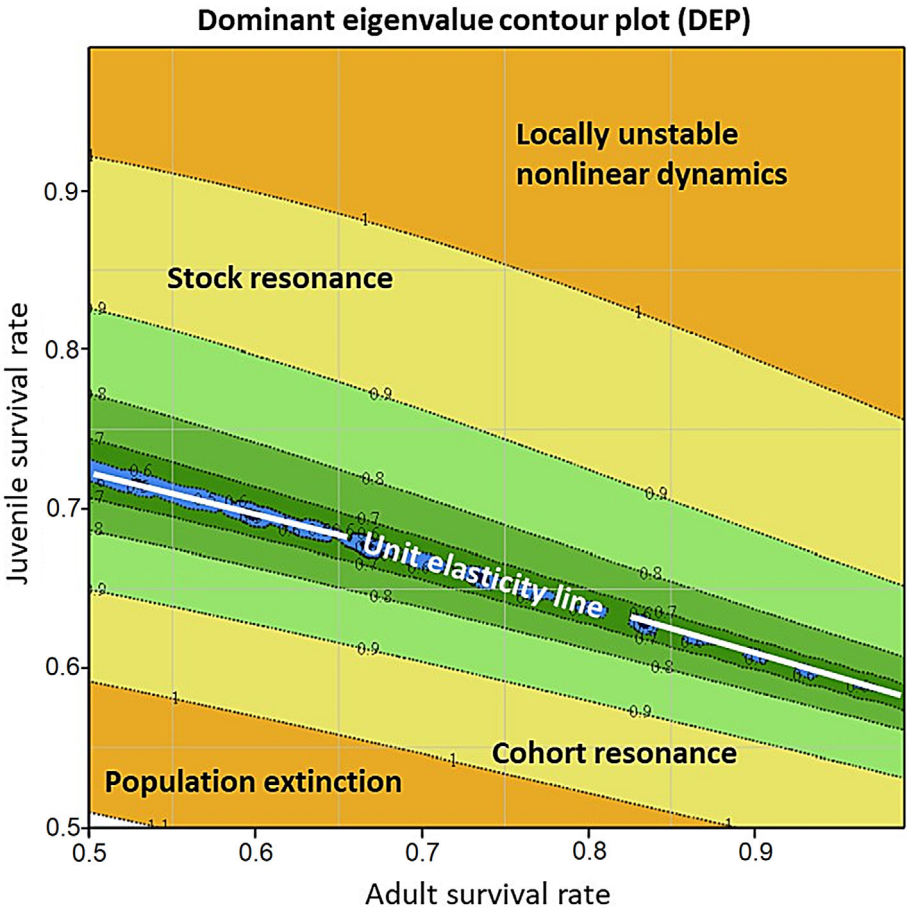

FIGURE 4 Map of dynamic regimes for populations with Moran–Ricker SRR ($a = 7, K = 1$) and life cycle with five immature and five mature cohorts. DEP coloration: Orange color—Dominant eigenvalue bigger than 1, yellow color—dominant eigenvalue between 0.9 and 1, green color—dominant eigenvalue between 0.5 and 0.9, blue color—dominant eigenvalue less than 0.5. The area below the unit elasticity line represents the elastic range of SRR (i.e., $|E_R| > 1$), while the area above represents the inelastic range of SRR (i.e., $|E_R| < 1$). The unit elasticity line defines by condition $|E_R| = 1$, or in the case of Moran–Ricker SRR by equation $LRS \equiv aL(\lambda_s, \lambda_y) = e$. Deviations from the unit elasticity line always reduce stability, more precisely, deviations toward greater elasticity can lead to extinction, while deviations toward greater inelasticity can lead to nonlinear instability [Color figure can be viewed at wileyonlinelibrary.com]

matrix depending on the parameters of the model. (2) The TF integral (contour) plot (TFIP), which shows the total variability of populations in response to environmental fluctuations depending on the parameters of the model and the spectrum of environment fluctuations. One example of the complementary use of these tools to identify and map dynamic regimes of the system is shown in Figures 4 and 5. In unstable regions (where the dominant eigenvalue is greater than 1), two regimes can be distinguished: (1) the population extinction regime, where $LRS \equiv aL < 1$ and (2) the locally unstable nonlinear regime, for which the linear approximation becomes invalid, and the population is involved in complex cyclic behavior. The stable region (where the dominant eigenvalue is lesser than 1) is divided on elastic and inelastic subregions by the unit elasticity line (defined by parametric equation $|E_R| = 1$). In the elastic subregion, on the border with the extinction regime, there is a zone of cohort resonance. In the inelastic subregion, at the boundary with the unstable nonlinear regime, there is the stock resonance zone. Both resonance zones can be clearly seen on TFIP as two stripes lying on the border between the stable and unstable regions, and TFIP can be used to mapping the stable regimes. In general, resonances occur at the boundaries of stable and unstable regimes, more precisely, cohort resonance at the border with population extinction, and stock resonance at the border with nonlinear instability. This feature of age-structured population behavior could be used as an early warning signal for extinction in the case of cohort resonance or population collapse (because of nonlinear instability) in the case of stock resonance. It should be noted that stability and variability are not always correlated properties of a population, for example, a decrease in stability does not necessarily lead to an increase in variability. Although, in some cases, such a negative correlation may be observed, the relationship between stability and variability is more convoluted and requires the combined use of both NAE and TF methods for evaluation.

5 | APPLICATIONS TO FISH STOCK MANAGEMENT

One of the important issues in fisheries management is how fishing pressure affects the sensitivity of stocks to environmental fluctuations (Gamelon et al., 2019). The TF approach allows explicit calculation of stock size variations in relation to the catch rate and from this calculate (objective) catch-dependent biological reference points as

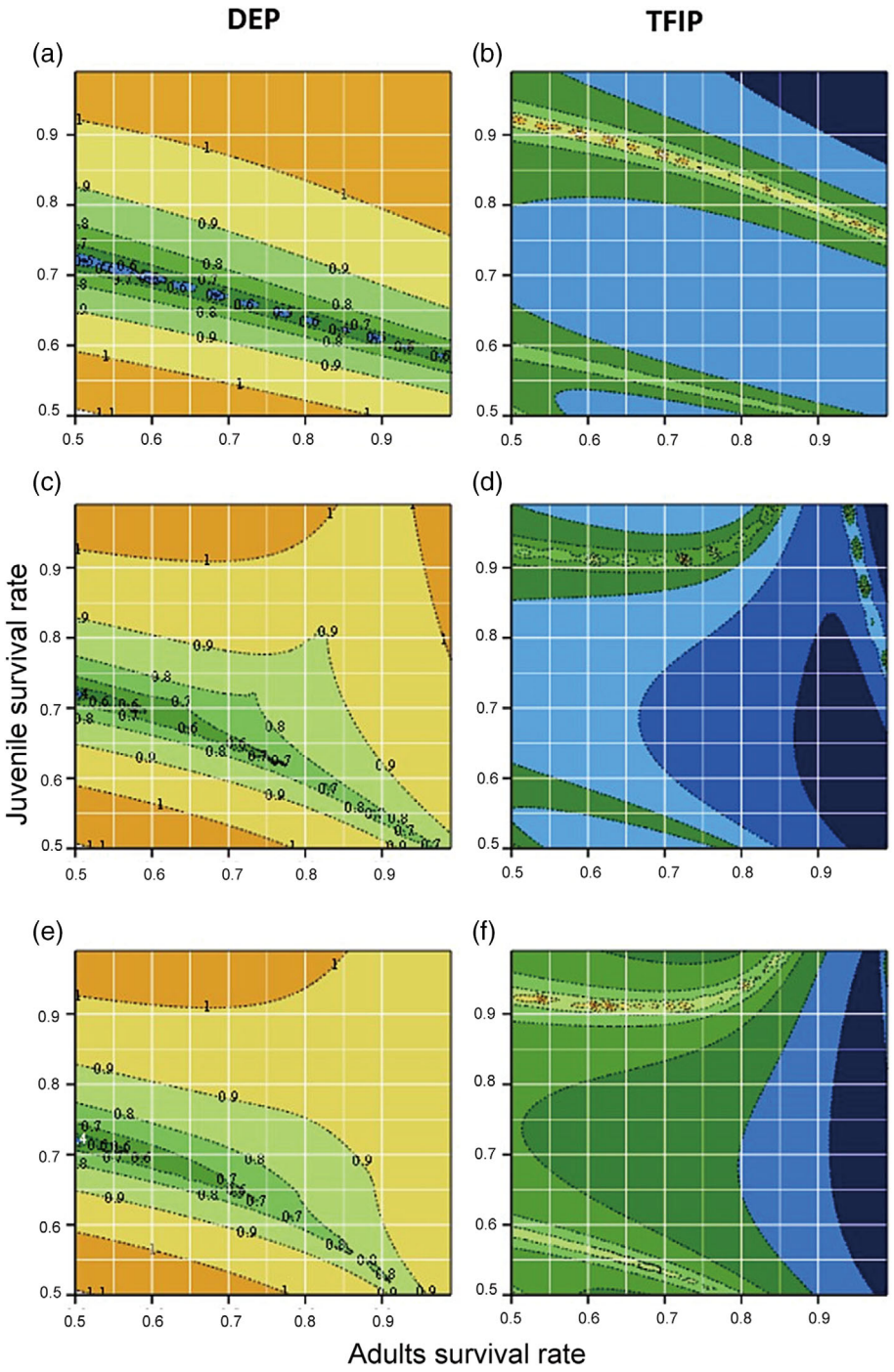

FIGURE 5 DEP (left, (a) (c) (e)) and corresponded TFIP (right, (b) (d) (f)) plots for populations with Moran–Ricker SRR ($a = 7$, $K = 1$) and life cycle with 5 immature and 5, 15 and 25 (from top to bottom) mature cohorts. All plots show juvenile survival on the vertical axis and adult survival on the horizontal axis. TFIP is colored in topographic colors, the upper yellow-orange stripe indicates the stock resonance, while the lower light green stripe indicates the cohort resonance [Color figure can be viewed at wileyonlinelibrary.com]

precautionary levels (in harvest control rules). In the case of a simple lifecycle (identical cohort reproductive quality, constant adult survival, absence of senescence), "white" environmental noise and unselective fishing on adult individuals, the variance of the stock can be written as

$$VarS(c) \sim 2 \cdot \int_0^{1/2} |TS(f, \lambda_s - c)|^2 df, \qquad (14)$$

where $c (c \le \lambda_s)$ is additional fishing mortality (or the catch rate). In order to estimate the integral (14) an estimation for the TF as a weighted sum of its limits can be used (Figure 3) $TS(f) \approx \lambda_s \cdot ITS(f) + (1 - \lambda_s) \cdot UTF(f)$ and then based on (11) and (13), the variance can be obtained as:

$$VarS(c) \sim (\lambda_s - c)^2 \cdot \frac{1 - \lambda_s + c}{1 + \lambda_s - c} + (1 - \lambda_s + c)^2 \cdot \frac{E_R(\lambda_s - c)^2}{m \cdot |2E_R(\lambda_s - c) + 1|}. \qquad (15)$$

This approximation provides an overall description of the *catch–stock variation relation*. The first term is a

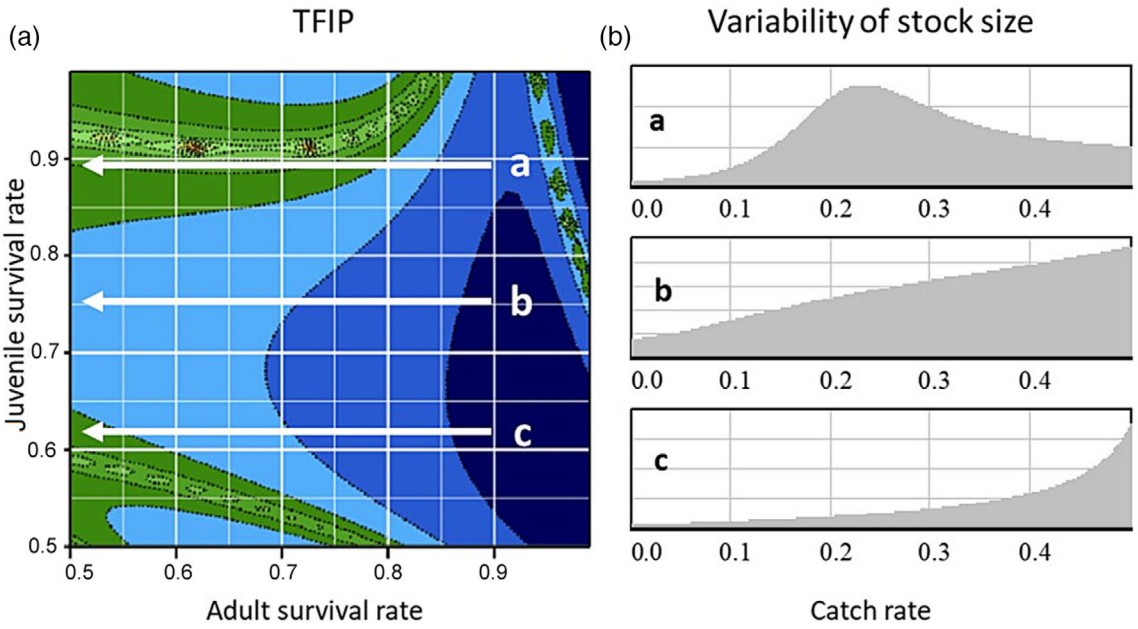

FIGURE 6 Catch–stock variation relations for populations with Moran–Ricker SRR ($a = 7$, $K = 1$) and life cycle with 5 immature and 15 mature cohorts. On the left panel (a), TFIP for adult versus juvenile survival rates is shown. White arrows show catch-induced changes in adult survival at three different values of juvenile survival rate (**a**: $\lambda_y = 0.89$, **b**: $\lambda_y = 0.75$, and **c**: $\lambda_y = 0.62$). On the right panel (b), cross-sections of the TFIP surface along lines a, b and c, each of which is specific catch–stock variation relation for the given juvenile survival rate. In case a, the stock resonance effect manifests itself as a hump in the middle of the catch range. In the case c, the cohort resonance appears as a sharp rise at high catch rates [Color figure can be viewed at wileyonlinelibrary.com]

monotonically increasing function of the catch, the second term depends on the elasticity (which in turn depends on the catch) and may have features associated with stock resonance. Using Table 2, explicit expressions for stock variations for different SRRs can be obtained. It may be noted that in the elastic range of any SRR, the stock variations increase with catch rate. One consequence of this is that for some classical SRR relations (Cushing and Beverton–Holt) for which the absolute value of elasticity is always greater than 1, the stock variations always grow with an increase in the catch and Equation (15) can be simplified to

$$VarS(c) \sim (\lambda_s - c)^2 \cdot \frac{1-\lambda_s+c}{1+\lambda_s-c} + (1-\lambda_s+c)^2 \cdot \frac{E_R(\lambda_s - c)}{2 \cdot m}. \tag{16}$$

Equation (14) or its approximation for specific SRR ranges (15 and 16) can be used to determine precautionary levels in the fishery (Hsieh et al., 2006; Subbey et al., 2014; Valpine & Hastings, 2002). Generally, the TF method allows us to obtain the catch–stock variation relation for any SRR, any lifecycle and any spectrum of environment noise by cross-sectioning of the TFIP surface along adult survival lines (Figure 6). Although the above analysis assumed unselective fishing, this restriction can be relaxed by using multiple TFIPs for different numbers of cohorts. To continue, applying Chebyshev's $\Pr(\Delta S(c)) \geq L_p \cdot \sqrt{VarS(c)}) \leq L_p^{-2}$, where $\Delta S(c)$ is deviation of stock log-size from its expected value at catch rate c and L_p is deviation level measured in standard deviation units. Accordingly, the bottom (lower limit) *precautionary level* is $\ln(S_P(c)) = \ln\left(\widehat{S}(c)\right) - L_p \cdot \sqrt{VarS(c)}$ or

$$S_P(c) = \widehat{S}(c) \cdot \exp\left(-L_p \cdot \sqrt{VarS(c)}\right), \tag{17}$$

where $\widehat{S}(c)$ is equilibrium stock size at catch rate c. Thus, Equation (17) along with Equations (15) and (16) make it possible to determine the values of precautionary levels for various catches and various levels of confidence. For example, if it is agreed (i.e., subjective) that the stock log-size should not be allowed below S_P with a probability of 95%, then a manager can set L_p to be approximately equal to 3 (reading from the Chebyshev's distribution). In practice, it may be useful to set a benchmark value for the precautionary level, for example, for catch corresponding to Maximum Sustainable Yield (MSY). In this case, the manager can calculate fishing mortality rate at MSY for a particular equilibrium stock size (Table 2) by solving the optimization equation $\widehat{S}(\lambda_s - c) + c \cdot \frac{\partial \widehat{S}(\lambda_s - c)}{\partial c} = 0$, which

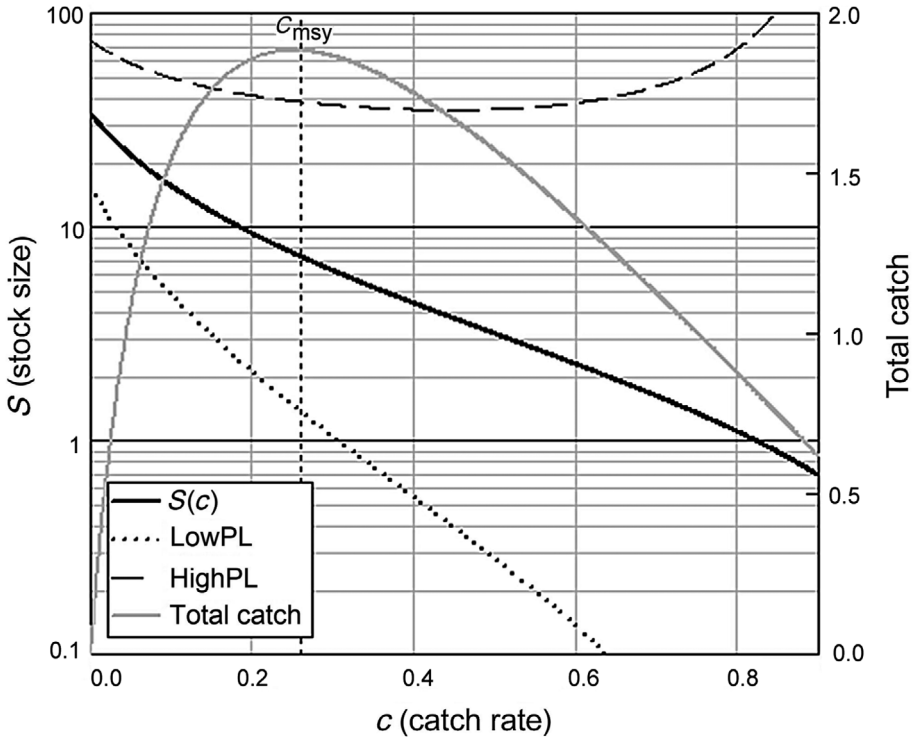

FIGURE 7 Example of fish stock control chart. On the main axis (log scale) are depicted: attractor (equilibrium) stock size (black line), basin of attraction depicted by bottom precautionary level (dotted line), and upper precautionary level (dashed line). Total catch (gray line) is shown on the secondary axis. Cmsy (vertical dotted line) shows catch rate corresponded to maximum sustainable yield (MSY). This is particular control cart for Beaverton–Holt SRR with parameters: $a = 3$, $K = 3$ and lifecycle with parameters: maturation age = 4, juvenile survival = 0.8, adult survival = 0.9

provides a value of c_{MSY} as well as the instantaneous rate of fishing mortality $F_{msy} \equiv -\ln(1 - c_{MSY})$ and MSY harvest $H_{MSY} = c_{MSY} \cdot \widehat{S}(\lambda_s - c_{MSY})$, and then substitute this value into Equation 17. For practical purposes, we recommend the use of a *fish stock control chart*, a graphical tool like Shewhart charts (Shewhart & Edwards-Deming, 1986), which is widely used for statistical process monitoring and quality control (Figure 7). Using this control chart, the manager can determine whether the exploited fish stock is under control (the current stock size is between the upper and lower precautionary levels) or not (otherwise additional managerial actions would be necessary).

6 | DISCUSSION

Uncertainty remains a serious problem in stock assessment and fisheries management generally. This is probably the most important motivation behind the use of precautionary reference levels in stock management. The "margin of safety" provided by these is debatable and constantly debated among stakeholders and managers. The frequency-response analysis developed here shows, for the first time, how precautionary reference levels can be objectively calculated from quantitative information describing the fish population in a few critical parameters. This is made all the more practical by our showing how the values depend on, and can be calculated for any given, or general, SRR. The fitting of stock-recruitment relations is notoriously difficult, so it is a major advantage to be able to assess uncertainty over a range of assumptions about them and indeed to generalize as we have done. This practical outcome of the analysis is made operational by using the fish stock control chart (Figure 7), or its software equivalent as a decision support tool for stock management.

Our analysis shows that one of the main sources of process uncertainty can be resonance phenomena in the age-structured population caused by environmental variations. An analytical description of the cohort resonance effect (increased sensitivity to environmental fluctuations at low frequencies and frequencies corresponding to the generation time) was made in the early 2000s (Bjørnstad & Nisbet, 2004) and was later confirmed by several empirical studies (Botsford et al., 2014; Gamelon et al., 2019; Rouyer et al., 2012). Cohort resonance takes place in the region of parameters adjacent to the population extinction regime, whereas the region of parameters adjacent to the locally unstable regime, which was classified according to the degree of stability as "*damped oscillations*" (Botsford et al., 2019), remained unexplored in terms of variability. Although, persistent population fluctuations arising in the locally unstable regime have been known since the 1950s (Barraquand et al., 2017; Botsford & Wickham, 1978; Ricker, 1954) under the name *2T-cycle* (or/and overcompensatory cycle), the fact that such persistent fluctuations can also occur within the stable region under the forcing of the environment variations deserves close attention and a special term—stock resonance. The essential difference

between these resonances is that cohort resonance is more of an amplification, whereas stock resonance is more of an accumulation of environment fluctuations. Since, in the first case, there is a significant correlation between environmental and population fluctuations, while in the second case, such a correlation may be absent. A more detailed description of the comparative properties of both resonances can be found in Table 4. It should be noted that, in contrast to cohort resonance, empirical evidence of stock resonance is still ambiguous, partly because the stock resonance regime and the nonlinear unstable oscillation regime are not easy to separate, therefore misattributions are possible. Moreover, a recent global study of 45 fish species (representing 222 fish stocks) showed that environmental fluctuations, rather than nonlinear dynamics, are the most likely cause of population fluctuations (Shelton & Mangel, 2011), thus stock resonance along with cohort resonance could be key hypotheses explaining population fluctuations.

We emphasize that a comprehensive understanding of age-structured population dynamics requires a combined analysis of stability (DEA method) and variability (TF method), which, as we showed above, are not necessarily mutually correlated properties. Using of these methods together avoids some overgeneralized conclusions. For example, on the top DEA-TFIP pair (Figure 5), we can see a liner diagonal pattern of regimes, suggesting the existence of a threshold value of elasticity, which defines the border between stable and unstable regimes (Botsford et al., 2019). In this special case, such a threshold value can be easily estimated as $|E_R| \approx 0.435$ (or $K \equiv E_S \approx -2.3$). However, with an increase in the number of cohorts, the pattern of regimes becomes more complicated (Figure 5, middle and bottom panels) and this threshold value of elasticity disappears. Similarly, based on the case of a small number of cohorts, someone might reasonably suggest that harvesting a population will tend to have a stabilizing effect on the dynamics (Botsford et al., 2019), but again, consideration of cases with an increased number of cohorts shows that this suggestion is not generally valid.

In particular, the TF method provides an analytical tool for exploring a variety of issues that have theoretical and practical importance (especially in quantifying the response of populations to environmental forcing). To facilitate its use, we have provided the MathCad code in the Supporting Information 1 and through the GitHub (Alexander-Sadykov/stock-resonance).

Considering the non-trivial relation between variations of stock sizes and catches (via adult survival) for age-structured populations, we can identify two difficulties for fish stock management based on MSY targets (alone). The first, we call "hyperopic vision"; it describes the situation were approaching an intended goal (e.g., MSY target) makes the goal more "blurred" (uncertain) due to increased stock variability, so that uncertainty in the detection of the MSY target increases (Figure 6, **c**). As one approaches the target, catch data for an intensively exploited stock may reveal more information about the background environmental fluctuations than about the stock dynamics itself because the vital parameters of the population become more uncertain, while the temporal population trends become more dictated by the environment (Pinsky & Byler, 2015). The second phenomenon, we term "blind-spot vision" depicts a situation where a slight change in catch within a certain range may invoke a sharp upsurge in the stock size variations due to stock resonance (Figure 6, **a**). That is, under certain conditions (inelastic range of SRR) there is a range of catch rates that could potentially lead to a stock collapse. In a sense, the TF approach provides some "spectacles," which may help with these difficulties. Hyperopic vision can be mitigated by establishing the catch-dependent precautionary levels, which may keep fishery pressure far enough from a "blurry" area, where the stock sizes and MSY targets become too uncertain. In addition, by using an explicit link between catch and stock variations, the manager can improve SRR curve fit by refitting the data considering the link between catch and uncertainty (Equation 17). The blind spot problem predicts a risk of unexpected collapse of stock under relatively low (compared MSY) fishery pressure due to the stock resonance effect. The TF approach can identify (for a particular stock) the conditions under which this effect may happen, and it is worth managers being aware of this danger. For example, stocks that follow Beverton–Holt or Cushing SRR do not have blind spots (free from stock resonance), while managing stocks that following Morran–Ricker SRR, or any other relation with low elasticity may present such a risk in which both increasing and decreasing fishery pressure can create resonance conditions. Since in practice there is usually considerable uncertainty over the underlying SRR (the curves are only best estimate statistical fits to often rather unclear data), the risk of losing control of a stock by stock resonance is potentially ever-present.

ACKNOWLEDGMENTS

This work was supported partially by Department of Agriculture, Food and the Marine (DAFM) (FishKOSM 487 project, DAFM reference 15/S/744).

CONFLICT OF INTEREST

Authors declare no conflict of interests.

ORCID

Alexander Sadykov https://orcid.org/0000-0002-0863-3887

REFERENCES

Anderson, C. N. K., Hsieh, C. H., Sandin, S. A., Hewitt, R., Hollowed, A., Beddington, J., May, R. M., & Sugihara, G. (2008). Why fishing magnifies fluctuations in fish abundance. *Nature*, *452*(7189), 835–839.

Barraquand, F., Louca, S., Abbott, K. C., Cobbold, C. A., Cordoleani, F., DeAngelis, D. L., Elderd, B. D., Fox, J. W., Greenwood, P., Hilker, F. M., Murray, D. L., Stieha, C. R., Taylor, R. A., Vitense, K., Wolkowicz, G. S. K., & Tyson, R. C. (2017). Moving forward in circles: Challenges and opportunities in modelling population cycles. *Ecology Letters*, *20*, 1074–1092.

Bjørnstad, O. N., & Nisbet, R. M. (2004). Trends and cohort resonant effects in age-structured populations. *Journal of Animal Ecology*, *73*, 1157–1167.

Botsford, L. W., Holland, M. D., Field, J. C., & Hastings, A. (2014). Cohort resonance: A significant component of fluctuations in recruitment, egg production, and catch of fished populations. *ICES Journal of Marine Science*, *72*(2), 285–296.

Botsford, L. W., White, J. W., & Hastings, A. (2019). *Population dynamics for conservation*. Oxford University Press.

Botsford, L. W., & Wickham, D. E. (1978). Behavior of age-specific, density-dependent models and the northern California Dungeness crab (*Cancer magister*) fishery. *Journal of the Fisheries Research Board of Canada*, *35*, 833–843.

Chavez, F. P., Ryan, J., Lluch-Cota, S. E., & Ñiquen, C. M. (2003). Climate: From anchovies to sardines and back: Multidecadal change in the Pacific Ocean. *Science*, *299*(5604), 217–221.

Gamelon, M., Sandercock, B. K., & Sæther, B. (2019). Does harvesting amplify environmentally induced population fluctuations over time in marine and terrestrial species? *Journal of Applied Ecology*, *56*, 2186–2194.

Gross, K., & de Roos, A. M. (2021). Resonance in physiologically structured population models. *Bulletin of Mathematical Biology*, *83*(8), 1–21.

Hill, M. (1973). Diversity and evenness: A unifying notation and its consequences. *Ecology*, *54*, 427–432.

Hixon, M. A., Johnson, D. W., & Sogard, S. M. (2014). BOFFFFs: On the importance of conserving old-growth age structure in fishery populations. *ICES Journal of Marine Science*, *71*, 2171–2185.

Hjort, J. (1914). Fluctuations in the great fisheries of northern Europe. Conseil Parmanent International Pour L'Exploration De La Mar. *Rapports et Proces-Verbaux*, *20*, 1–228.

Hjort, J. (1926). Fluctuations in the year classes of important food fishes. *Journal du Conseil International Pour l'Explora- tion de la Mer*, *1*, 5–38.

Hsieh, C. H., Reiss, C. S., Hunter, J. R., Beddington, J. R., May, R. M., & Sugihara, G. (2006). Fishing elevates variability in the abundance of exploited species. *Nature*, *443*(7113), 859–862.

Myers, R. A., Bowen, K. G., & Barrowman, N. J. (1999). Maximum reproductive rate of fish at low population sizes. *Canadian Journal of Fisheries and Aquatic Sciences*, *56*(12), 2404–2419.

Paniw, M., Ozgul, A., & Salguero-Gómez, R. (2018). Interactive life-history traits predict sensitivity of plants and animals to temporal autocorrelation. *Ecology Letters*, *21*(2), 275–286.

Pinsky, M. L., & Byler, D. (2015). Fishing, fast growth and climate variability increase the risk of collapse. *Proceedings of the Royal Society B: Biological Sciences*, *282*, 20151053.

Ricker, W. E. (1954). Stock and recruitment. *Journal of the Fisheries Research Board of Canada*, *11*, 559–623.

Ripa, J., & Lundberg, P. (1996). Noise colour and the risk of population extinctions. *Proceedings of the Royal Society B: Biological Sciences*, *263*, 1751–1753.

Ripa, J., Lundberg, P., & Kaitala, V. (1998). A general theory of environmental noise in ecological food webs. *American Naturalist*, *151*, 256–263.

Rouyer, T., Sadykov, A., Ohlberger, J., & Stenseth, N. C. (2012). Does increasing mortality change the response of fish populations to environmental fluctuations? *Ecology Letters*, *15*(7), 658–665.

Royama, T. (1992). *Analytical population dynamics*. Chapman & Hall.

Schmidt, A. E., Botsford, L. W., Patrick Kilduff, D., Bradley, R. W., Jahncke, J., & Eadie, J. M. (2018). Changing environmental spectra influence age-structured populations: Increasing ENSO frequency could diminish variance and extinction risk in long-lived seabirds. *Theoretical Ecology*, *11*, 367–377. https://doi.org/10.1007/s12080-018-0372-5

Schwartzlose, R. A., Alheit, J., Bakun, A., Baumgartner, T. R., Cloete, R., Crawford, R. J. M., Fletcher, W. J., Green-Ruiz, Y., Hagen, E., Kawasaki, T., Lluch-Belda, D., Lluch-Cota, S. E., MacCall, A. D., Matsuura,Y., Nevárez-Martínez, M. O., Parrish R. H., Roy, C., Serra, R., Shust, K. V., Ward M. N., & Zuzunaga, J. Z. (1999). Worldwide large-scale fluctuations of sardine and anchovy populations. *South African Journal of Marine Science*, *21*, 289–347.

Shelton, A. O., & Mangel, M. (2011). Fluctuations of fish populations and the magnifying effects of fishing. *Proceedings of the National Academy of Sciences of the United States of America*, *108*(17), 7075–7080.

Shewhart, W. A., & Edwards-Deming, W. (1986). *Statistical method from the viewpoint of quality control*. Dover Publications.

Solari, A. P., Santamaría, M. T. G., Borges, M. F., Santos, A. M. P., Mendes, H., Balguerias, E., Díaz Cordero, J. A., Castro, J. J., & Bas, C. (2010). On the dynamics of *Sardina pilchardus*: Orbits of stability and environmental forcing. *ICES Journal of Marine Science*, *67*(8), 1565–1573.

Subbey, S., Devine, J. A., Schaarschmidt, U., & Nash, R. D. M. (2014). Modelling and forecasting stock–recruitment: Current and future perspectives. *ICES Journal of Marine Science*, *71*(8), 2307–2322.

Valpine, P. D. E., & Hastings, A. (2002). Fitting population models incorporating process noise and observation error. *Ecological Monographs*, *72*(1), 57–76.

Willberg, M. J., Woodward, R. T., Huang, P., & Tomberlin, D. (2019). Developing precautionary reference points for fishery management using robust control theory: Application to the Chesapeake Bay blue crab *Callinectes sapidus* fishery. *Marine and Coastal Fisheries: Dynamics, Management, and Ecosystem Science*, *11*, 177–188.

SUPPORTING INFORMATION

Additional supporting information may be found in the online version of the article at the publisher's website.

How to cite this article: Sadykov, A., Farnsworth, K., Sadykova, D., & Stenseth, N. C. (2022). The transfer function method reveals how age-structured populations respond to environmental fluctuations with serious implications for fisheries management. *Population Ecology*, *64*(3), 190–204. https://doi.org/10.1002/1438-390X.12124